J Herbmed Pharmacol. 2023; 12(2): 283-298.

http://www.herbmedpharmacol.com doi: 10.34172/jhp.2023.31

Journal of Herbmed Pharmacology

In vitro and *in silico* investigation of garlic's (*Allium sativum*) bioactivity against 15-lipoxygenase mediated inflammopathies

Arman Mahmud Khan[1#], Md. Arman Sharif[1#], Rahagir Salekeen[1], Md. Hafijur Rahman[1], Sakib Mahmud[1], Partha Biswas[2], Md. Nazmul Hasan[2], Kazi Mohammed Didarul Islam[1], Md. Morsaline Billah[1], Md. Emdadul Islam[1*]

[1]Biotechnology and Genetic Engineering Discipline, Life Science School, Khulna University, Khulna-9208, Bangladesh
[2]Department of Genetic Engineering and Biotechnology, Jashore University of Science and Technology, Jashore-7408, Bangladesh
[#] These authors contributed equally to this study.

ARTICLE INFO

Article Type:
Original Article

Article History:
Received: 30 August 2022
Accepted: 17 October 2022

Keywords:
Antioxidant
Anti-inflammatory agents
Anticoagulant
Inflammation
Phenolic compounds

ABSTRACT

Introduction: Garlic (*Allium sativum*) is widely used as a flavor-enhancing dietary ingredient and exhibits a wide spectrum of pharmacological effects. This study aimed to investigate the therapeutic effects of aqueous garlic extract to explore the bioactivity against 15-lipoxygenase (15-LOX) mediated inflammopathies.

Methods: In this study, the antioxidant (DPPH free radical scavenging assay and reducing power assay), anti-inflammatory (hypotonicity-induced hemolysis assay and 15-LOX inhibition assay) and anticoagulation (serine protease inhibition assay and prothrombin time assay) effects of the aqueous garlic extract were investigated. Furthermore, in silico molecular docking and dynamic simulation analysis of reported small compounds of garlic against 15-LOX1 and 15-LOX2 were performed to figure out the most efficient phytochemical ligands and validate the anti-inflammatory potential.

Results: The DPPH scavenging effect and the reducing power of the extract were found with the IC_{50} of 213.87 ± 1.49 μgmL^{-1} and EC50 of 124.78 ± 3.39 μgmL^{-1}, respectively. In the hypotonicity-induced hemolysis and 15-LOX inhibition assay, the IC50 values were observed as 147.59 ± 2.98 μgmL^{-1} and 250.05 ± 8.48 μgmL^{-1}, respectively. The extract inhibited serine protease activity with an IC50 of 301.33 ± 1.31 μgmL^{-1} and prevented blood coagulation for 10.05 ± 0.35 minutes in prothrombin time assay. The *in silico* study identified Rhamnetin as a potential 15-LOX1 and 15-LOX2 inhibitor, and it exhibited a stable interaction with the targets throughout the 100 ns dynamic simulation.

Conclusion: The findings of this study provide molecular insights into garlic's medicinal properties as well as its bioactive compounds, which can be potential therapeutic interventions for 15-LOX mediated inflammations.

Implication for health policy/practice/research/medical education:
The findings of this study suggest that bioactive compounds of garlic extract have potent therapeutic features as anti-inflammatory agents that can help to explore and investigate new potentially active therapeutics from garlic against lipoxygenase mediated chronic inflammatory illness.

Please cite this paper as: Khan AM, Sharif MA, Salekeen R, Rahman MH, Mahmud S, Biswas P, et al. *In vitro* and *in silico* investigation of garlic's (*Allium sativum*) bioactivity against 15-lipoxygenase mediated inflammopathies. J Herbmed Pharmacol. 2023;12(2):283-298. doi: 10.34172/jhp.2023.31.

Introduction

Reactive oxygen species (ROS) are formed as byproducts of metabolic processes inside the cells and contribute to maintaining cellular redox homeostasis (1). Despite ROS being necessary for microbial resistance and cell signaling pathways, these free radicals are also commonly regarded as potentially toxic reactive agents owing to their ability to alter important cellular components. These highly reactive and unstable radicals are ready to oxidize proteins, nucleic acids, carbohydrates, lipids, and other biological macromolecules, initiating a chain of events that subsequently leads to cell death and severe tissue damage (2). Excessive ROS synthesis disrupts cellular homeostasis and triggers oxidative stress, which

***Corresponding author**: Md. Emdadul Islam,
Email: emdad@bge.ku.ac.bd

contributes to lipid peroxidation in biomembranes and induces severe inflammatory pathways, thereby accelerating the progression of several pathophysiological illnesses (3). Furthermore, elevated ROS level activates oxidative enzymes like lipoxygenases (LOXs) that catalyze the oxidation of free polyunsaturated fatty acids (PUFAs) to synthesize hydroperoxides, which are implicated in the molecular pathogenesis of many chronic inflammatory diseases (4). 15-LOX modulates the oxidative alternation of low-density lipoproteins (LDLs) and generates pro-inflammatory leukotrienes that subsequently trigger the emergence of atherosclerotic lesions (5). Antioxidants can retard ROS-mediated oxidative damage by neutralizing the free radicals and preventing lipid peroxidation, thereby arresting the onset of a wide spectrum of chronic diseases.

Plant-derived metabolic constituents such as polyphenolics, carotenoids, and vitamins are natural antioxidants that manifest prominent therapeutic effects, including antimicrobial, anti-inflammatory, anticancer, and antitumor activities (6). Garlic (*Allium sativum*) is commonly known as an aromatic spice, which is extensively used as a food additive due to its distinct flavor and potential therapeutic benefits. It has traditionally been utilized both for culinary and medicinal purposes in many cultures (7). It is now regarded as one of the most efficacious disease-preventive dietary ingredients that exhibits a wide spectrum of pharmacological effects; for instance, antiatherosclerosis, hypolipidemic, hypoglycemic, anticoagulation, anticancer, chemopreventive, antimicrobial, and hepatoprotective activities (8-10). Garlic is reported to be rich in natural bioactive compounds that act as antioxidants, lower ROS levels in the body, and prevent the oxidation of LDL (11). Furthermore, garlic extract has been advocated to have potent prophylactic effects against oxidative stress, endothelial dysfunction, thrombosis, high blood cholesterol levels, and the progression of chronic heart diseases (12). The health-promoting effects of garlic are substantially attributed to its predominant organo-sulfur compounds; for instance, alliin, allicin, S-allyl cysteine, diallyl sulfide, diallyl disulfide, allyl mercaptan, along with other phytochemical constituents (e.g., phenolics, flavonoids, tannins, terpenoids, saponins, anthocyanins, vitamins, fatty acids, and so on (13-17). Considering garlic's therapeutic features, this study aimed to determine the antioxidant, anti-inflammatory, and anticoagulant properties of aqueous garlic extract to explore the bioactivity against 15-LOX mediated inflammopathies and evaluate its effectiveness when used in traditional culinary purposes.

Materials and Methods

Sample collection and extract preparation

Fresh garlic bulbs were purchased from Gollamari Bazar, Khulna, on November 21, 2021. The sample was then taxonomically identified and a voucher specimen (Accession Number: AA-KU-2021019) was submitted to the herbarium of the Forestry and Wood Technology Discipline, Khulna University, Khulna-9208, Bangladesh. The bulbs were cleaned thoroughly, isolated from unwanted impurities, and chopped into fine small flakes. The small flakes were allowed to dry in the shade and open air for a few days. After drying, the flakes were pulverized into a fine powder with a grinder. The powder was then weighed and kept in sealed plastic bags for further use. The powdered garlic bulbs were then placed in a clean, flat-bottomed glass jar and extracted with water (1:5 w/v) for seven days at ambient temperature, with periodic stirring and shaking. The mixture was filtered through a fresh white cloth along with Whatman filter paper no. 41 to remove coarse plant materials and the filtrate was air-dried at room temperature to yield water extract, which was used for further *in vitro* experiments.

Blood collection

From fifteen healthy participants who were not taking any antiplatelet medications, 5 mL of blood sample was drawn from each donor following the blood collection procedure of the Bangladesh Medical Research Council. The blood samples were then immediately transferred to EDTA tubes to inhibit coagulation. Before collecting the blood sample, an earlier informed written consent, ethical code: KUAEC-2017/08/14 of the Khulna University Research Cell, was taken from all the participants.

Determination of antioxidant activity

DPPH free radical scavenging activity assay

The effectiveness of the garlic extracts in preventing oxidation was evaluated by 2,2-diphenyl-1-picrylhydrazyl (DPPH) scavenging assay (18). The garlic extract and standard solution of Ascorbic acid were serially diluted to make aliquots of seven different concentrations (400 to 6.25 µg/mL). One milliliter of each concentration was mixed with an equal volume of freshly prepared 0.004% (w/v) DPPH methanolic solution and the absorbance of each tube was measured at 517 nm after incubating at room temperature for 30 minutes in the dark. The percentage of inhibition was estimated as equation (1):

$$\%\text{Inhibition} = \frac{(Absorbance\,of\,blank - Absorbance\,of\,sample)}{Absorbance\,of\,blank} \times 100$$

Reducing power assay

The reducing power assay of the extract was carried out according to (19). The garlic extract and standard solution of Ascorbic acid were serially diluted to make aliquots of seven different concentrations (400 to 6.25 µg/mL). one ml of each concentration was added to 2.5 mL of phosphate buffer (0.2 M, pH = 6.6) and 1% potassium ferricyanide [$K_3Fe(CN)_6$] and allowed to stand for 20 minutes. Following that, the reaction mixture was mixed with 2.5 mL of 10% trichloroacetic acid (TCA) and

centrifuged for 10 minutes at 3000 rpm. The blank was prepared similarly to the sample, except that no extract or standard was added. The reaction mixture's higher absorbance revealed an elevated reducing power.
The percent increase in reducing power was determined as equation (2):

$$\%\text{Reduction} = \frac{(Absorbance\,of\,blank - Absorbance\,of\,sample)}{Absorbance\,of\,blank} \times 100$$

Quantitative determination of antioxidant molecule

Total phenolic content

The total phenolic content (TPC) of aqueous garlic extract was determined by Folin-Ciocalteu (FC) colorimetric assay (20), wherein, 1 mL of sample (100 µg/mL) or standard gallic acid solution (6.25 to 200 µg/mL) was added to 9 mL of distilled water, followed by 1 mL of FC reagent (diluted 10 times). After 5 minutes, 10 mL of 7% Na_2CO_3 and distilled water were added to make a total volume of 25 mL and left to incubate for 60 minutes in the dark. Following the incubation, the absorbance was measured at 750 nm. The TPC was measured from the standard calibration curve as gallic acid equivalents (GAE) in mg/g of extract.

Total flavonoid content

The total flavonoid content (TFC) of garlic extract was measured as a previously described procedure of aluminum chloride colorimetric assay (20). 5% $NaNO_2$ (0.3 mL) was combined with 1 mL of garlic extract (100 µg/mL) followed by 5 mL distilled water and kept for 5 minutes. The reaction mixture was then mixed with 0.6 mL of 10% $AlCl_3$ and 2 mL of NaOH (1 M) and incubated at ambient temperature for 5 minutes. Following that, the absorbance was measured at 510 nm. Different concentrations of standard quercetin solution (400 to 25 µg/mL) were used to construct the standard calibration curve. The TFC was measured from the quercetin calibration curve as quercetin equivalents (QE) in mg/g of extract.

Total tannin content

The total tannin content (TTC) was measured using the procedure reported previously (20). One milliliter of sample extract (100 µg/mL) was combined with 0.5 mL of FC reagent and 7.5 mL of distilled water and kept for 5 minutes in the dark. Afterward, 1 mL of 35% Na_2CO_3 solution was mixed with the solution and the total volume was made to 10 mL with distilled water. The entire solution was further left to stand at ambient temperature for 30 minutes. Following the incubation, the absorbance was taken at 725 nm. Different concentrations of standard gallic acid solution (200 to 3.125 µg/mL) were used to construct the standard calibration curve. The TTC was measured from the calibration curve as GAE in mg/g of extract.

Determination of anti-inflammatory activity

Hypotonicity-induced hemolysis assay

Hypotonicity-induced hemolysis assay was conducted to determine the ex-vivo anti-inflammatory activity of garlic extract according to (21) with some adjustments. The hypotonic solution was used to investigate the lysis of human RBC in this assay. The collected blood samples were centrifuged for 5 minutes at 3000 rpm, and the supernatant was discarded carefully. The precipitated RBC part was centrifuged three times at 2500 rpm for 5 mins with sterile washing buffer (0.9% NaCl). Following that, an RBC suspension with a concentration of 10% (v/v) was prepared with 10 mM phosphate buffer solution. The isotonic solution was prepared by dissolving 154 mM sodium chloride in 10 mM phosphate buffer solution and the pH was adjusted to 7.4. The sample and standard (Aspirin) were serially diluted to phosphate buffer solution to make aliquots of five different concentrations (400 to 25 µg/mL). After that, 600 µL of sample or standard and 600 µL of RBC suspension were mixed with 600 µL of isotonic solution in a 2 mL Eppendorf tube. Likewise, the hypotonic solution was mixed with RBC suspension and sample or standard solution. The mixture contained only RBC and the hypotonic solution was considered as control. The entire combination was then kept for 10 minutes at 37°C. Following incubation, the reaction mixture was centrifuged for 15 minutes at 5000 rpm, and the optical density (OD) of the supernatant was determined at 540 nm. The percent inhibition of hemolysis was determined as equation (3):

$$\%Inhibition\,of\,hemolysis = 1 - \frac{(OD2 - OD1)}{(OD3 - OD1)} \times 100$$

Where OD1 indicates sample in isotonic solution, OD2 indicates sample in the hypotonic solution, and OD3 indicates control sample in the hypotonic solution.

15-Lipoxygenase (15-LOX) inhibition assay

The sample extract was evaluated for LOX inhibition activity using lyophilized soybean 15-LOX according to Wangensteen's procedure (22) with a few adjustments. 975 µL 15-LOX solution (3000 U/mL; reconstituted with 0.2M borate buffer; pH 9.0) was mixed to 25 µL of different concentrations (50 to 400 µg/mL) of sample extract, standard (Quercetin), or blank (0.1 M PBS solution). An extra double blank (25 µL 0.1 M PBS solution + 975 µL borate buffer) was made without enzyme as a control. Then, each tube was combined with 517.5 µM linoleic acid substrate solution (reconstituted with 0.2 M borate buffer with pH 9.0) to initiate the enzymatic reaction. The absorbance of the reaction mixture was determined at one-minute intervals for five minutes. For each concentration, the absorbance vs. time plot was prepared (ΔAbsorbance/ΔTime) and the slope for enzyme inhibition was calculated as equation (4):

$$\%\text{Inhibition} = \frac{\text{Slope}\left(\frac{\Delta\text{Absorbance}}{\Delta\text{Time}}\right)_{\text{Blank}} - \text{Slope}\left(\frac{\Delta\text{Absorbance}}{\Delta\text{Time}}\right)_{\text{Sample}}}{\text{Slope}\left(\frac{\Delta\text{Absorbance}}{\Delta\text{Time}}\right)_{\text{Blank}}}$$

Determination of anticoagulant activity

Serine protease inhibition assay

Serine protease inhibition assay was conducted based on a previously described procedure (23). The sample and standard (Quercetin) were serially diluted to make aliquots of five different concentrations (400 to 25 µg/mL). From each concentration, 250 µL of sample and standard was transferred into a 2 mL Eppendorf tube. After that, 250 µL of 0.05% Trypsin solution (preheated for 15 minutes at 37°C) and 500 µL of 1% casein (prepared in 0.1 M phosphate buffer) were added to each reaction tube. Afterward, the entire solution was left to keep for 30 minutes at 37°C. Then, 3 mL of 5% TCA solution was mixed to arrest the reaction and centrifuged at 12,000 rpm for 15 minutes. The absorbance of the supernatant was measured at 280 nm and the percent inhibition of serine protease was calculated as equation (5):

$$\%\text{Inhibition} = \frac{(Absorbance\ of\ sample - Absorbance\ of\ blank)}{Absorbance\ of\ sample} \times 100$$

Prothrombin time (PTT) assay

The PTT assay was performed following the procedure reported previously by (24). From the collected blood samples, the plasma was carefully separated from each blood sample after centrifuging for 15 minutes (3000 rpm). The plasma was then stored at 4°C until it was used. 200 µL of plasma was mixed with 100 µL of various concentrations (800 to 50 µg/mL) of standard (Warfarin) and garlic extract, followed by a gentle vortex for appropriate mixing. Afterward, 300 µL of $CaCl_2$ (25 mM) was mixed into each reaction tube and the entire mixture was allowed to keep in the water bath at 37°C. The time required for the sample and standard to coagulate was estimated over a 5-second interval.

Statistical analysis

All *in vitro* biochemical assays were conducted in triplicate for each concentration and negative control under the same environmental parameter. In all experiments, the percent inhibition of each concentration was statistically compared to the negative control to evaluate the level of significance using the one-tailed *t* test with corresponding *P* values: 0.12 (ns), 0.033 (*), 0.002 (**), and 0.001 (***). The linear relationship for each dependent variable was further analyzed using the Pearson correlation test, where the R^2 value close to 1 indicates a strong relationship. GraphPad Prism 9.3.1 software was used for all statistical analyses.

In silico study

Target protein retrieval and preparation

15-LOX2 crystal structure (PDBid:4NRE) was retrieved from protein data bank repositories. On the other hand, the 15-LOX1 structure was generated using the 'HHpred server' from its FASTA sequence (Accession No: P16050.3) (25). The constructed structure was then validated through the Ramachandran plot using Procheck (26).

Phytochemical library preparation and molecular docking study

A phytochemical library of previously reported 89 compounds from garlic was prepared through an extensive literature review wherein the compounds were identified through several mass spectrometric analyses. Afterward, UCSF Chimera was employed for molecular optimization of selected ligands and target proteins (15-LOX1 and 15-LOX2) (27). PyRx (version 0.8) was then used to assess the binding energy of these compounds with 15-LOX2 (PDB ID: 4NRE) and 15-LOX1 (28). The renowned anti-inflammatory drug, Ibuprofen (PubChem CID-3672), was taken as the control drug for the *in silico* study (29). Following the molecular docking study, hydrogen bonds and hydrophobic interactions of protein-ligand (P-L) complexes were investigated through LigPlot+ software (version 2.2.4) (30).

Physicochemical and drug-likeness properties analysis

Following the docking analysis, the top scoring ligands were investigated for physicochemical properties and Absorption, Distribution, Metabolism, Excretion, and Toxicity (ADMET) using pkCSM and the Swiss-ADME server (30,31). After analyzing drug-likeness properties, the top three potential lead molecules for each target were selected for the molecular dynamic simulation (MDS) study.

Molecular dynamic simulation study

MDS was performed for 100 nanoseconds (ns) to evaluate the stability of the P-L complexes using the Linux-based "Desmond v3.6 Program". The stability and effective binding of P-L complexes were evaluated by the analysis of P-L contacts, root mean square deviation (RMSD), root mean square fluctuation (RMSF), radius of gyration (Rg), and intramolecular hydrogen bonds (32).

Results

Determination of antioxidant activity

DPPH free radical scavenging assay

The inhibitory activity of DPPH free radical scavenging enhanced linearly with increasing concentration (Figure 1A). The percent inhibition of DPPH scavenging at 400 μgmL^{-1} concentration of the aqueous extract was determined to be 65.51%, compared to the reference standard ascorbic acid (72.57%). The aqueous extract demonstrated significant ($P < 0.001$) antioxidant potential with the half maximal inhibitory concentration (IC_{50}) of $213.87 \pm 1.49\ \mu gmL^{-1}$, whereas the standard ascorbic acid possessed the IC_{50} of $130.53 \pm 2.62\ \mu gmL^{-1}$ (Figure 1B).

Reducing power assay

The aqueous extract and the standard ascorbic acid demonstrated a higher reducing power, which elevated in a concentration-dependent linear pattern (Figure 1C). The aqueous extract exhibited a significant ($P < 0.001$) reducing potential with a comparatively lower half maximal effective concentration (EC_{50}) of 124.81 ± 3.39 μgmL^{-1} in comparison to reference standard ascorbic acid (EC_{50} = 33.83 ± 2.68 μgmL^{-1}) (Figure 1D).

Quantitative determination of antioxidant molecule

Total phenolics, flavonoid and tannin content

The TPC and TTC of the extract were quantified as mg GAE/g of extract, whereas TFC was quantified as mg QE/g of extract. The extract exhibited a substantial amount of phenolic acid (306.77 ± 1.53 mg GAE/g dry extract), flavonoid (252.22 ± 1.09 mg QE/g dry extract) and tannin (87.50 ± 0.99 mg GAE/g dry extract) content.

Determination of anti-inflammatory activity

Hypotonicity-induced hemolysis assay

The aqueous extract of garlic could significantly ($P < 0.001$) protect the RBC membrane from hypotonicity-induced hemolysis in a concentration-dependent linear pattern (Figure 2A). The percent inhibition of hemolysis at 400 μgmL^{-1} concentration of the aqueous extract was 71.70%, compared to standard aspirin (92.23%). The extract demonstrated substantial inhibitory activity with an IC_{50} of 147.59 ± 2.98 μgmL^{-1}, whereas aspirin possessed an IC_{50} of 59.08 ± 3.02 μgmL^{-1} (Figure 2B).

15-LOX inhibition assay

The 15-LOX inhibition activity of the aqueous extract revealed a dose-dependent inhibition of the linoleic acid peroxidation by soybean 15-LOX, which is used as a model for mammalian LOXs (Figure 2C). The highest percent inhibition at 400 μgmL^{-1} concentration of the aqueous extract was 72.46%, compared to standard Quercetin (96.76%). The aqueous extract demonstrated substantial inhibitory activity with an IC_{50} of 250.05 ± 8.48 μgmL^{-1}, whereas Quercetin possessed an IC_{50} of 19.62 ± 6.52 μgmL^{-1} (Figure 2D).

Determination of anticoagulant activity

Serine protease inhibition assay

The aqueous extract inhibited the proteolytic degradation of casein, which was catalyzed by the serine protease (trypsin) in a concentration-dependent pattern (Figure 3A). The highest percent inhibition at 400 μgmL^{-1} concentration of the aqueous extract was 57.22%, compared to standard Quercetin (70.77%). The extract manifested significant ($P < 0.001$) protease inhibitory activity with an IC_{50} of 301.33 ± 1.31 μgmL^{-1}, whereas Quercetin possessed an IC_{50} of 218.29 ± 6.58 μgmL^{-1} (Figure 3B).

PTT assay

The aqueous garlic extract exhibited strong inhibition of plasma clot formation in a concentration-dependent pattern. The aqueous extract at 800 μgmL^{-1} required 10.05 ± 0.35 minutes to coagulate the plasma, whereas the standard drug (warfarin) at 800 μgmL^{-1} needed 23.78 ± 0.44 minutes to complete the coagulation (Figure 3C).

Correlations among antioxidant, anti-inflammatory, and anticoagulation activities

Linear correlation was found among antioxidant, anti-

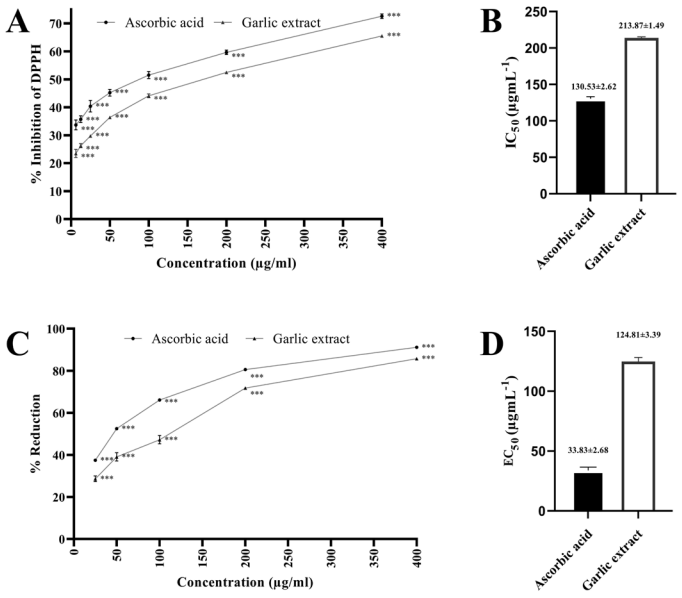

Figure 1. Antioxidant activity of aqueous garlic extract and ascorbic acid (standard): (A) percent inhibition of DPPH free radical; (B) the half maximal inhibitory concentration (IC_{50}) value (μgmL^{-1}) of DPPH scavenging assay; (C) percent reduction in reducing power assay; (D) the half maximal effective concentration (EC_{50}) value (μgmL^{-1}) of reducing power; (*** indicates $P < 0.001$ compared to the control group).

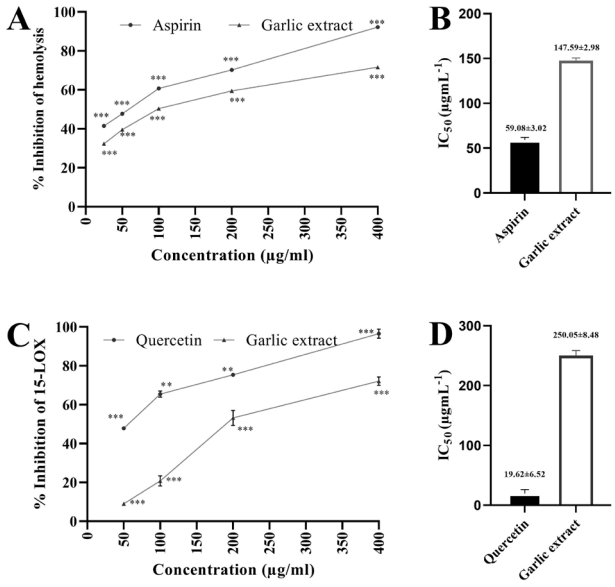

Figure 2. Anti-inflammatory activity of aqueous garlic extract and standards: (A) percent inhibition of hemolysis; (B) the half maximal inhibitory concentration (IC_{50}) value (µgmL^{-1}) of hemolysis; (C) percent inhibition of 15-lipoxygenase (15-LOX); (D) IC_{50} (µgmL^{-1}) value of 15-LOX inhibition; (** indicates $P < 0.002$ and *** indicates $P < 0.001$ compared to the control group).

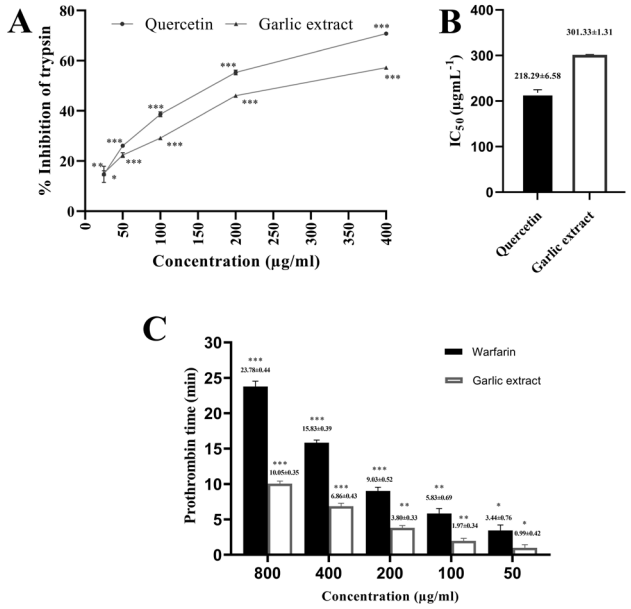

Figure 3. Anticoagulation activity of aqueous garlic extract and standards: (A) percent inhibition of serine protease; (B) the half maximal inhibitory concentration (IC_{50}) value (µgmL^{-1}) of protease inhibition; (C) prothrombin time of garlic extract and warfarin (standard); (* indicates $P < 0.033$; ** indicates $P < 0.002$ and *** indicates $P < 0.001$ compared to the control group).

inflammatory, and anticoagulation activity of aqueous garlic extract. The R^2 values for DPPH free radical scavenging, reducing power, hypotonicity-induced hemolysis, and serine protease inhibition assay ranged between 0.80 and 0.95, although the PTT assay did not correlate strongly with any of the other assays (Figure 4).

In silico study

Structure validation of 15-LOX1

15-LOX1 structure was constructed through HHpred and validated through Procheck server (Figure 5). The Ramachandran plot of excellent quality structure assures that more than 90% of the residues are in the favorable zone (33). The plot statistics of the contracted 3d structure showed 93.7% (534) residues in most favored position (A, B, L) and the rest of the residues (36) were in additional allowed regions (a, b, l, p).

ADMET profiling and visualization

Following the comprehensive docking, 12 phytochemicals

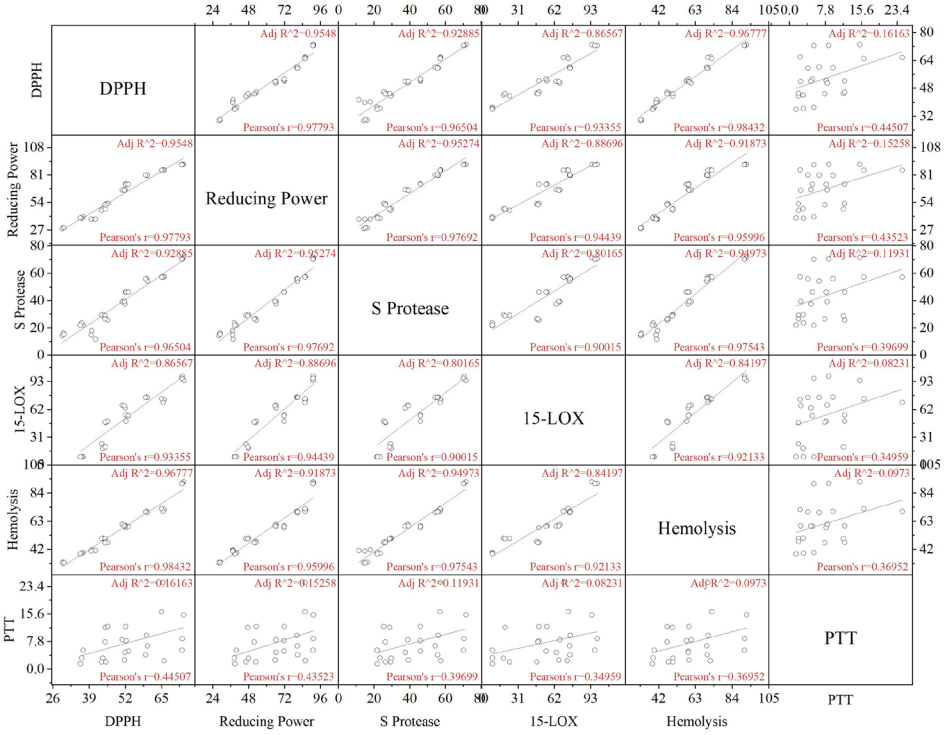

Figure 4. Correlations among antioxidant activities: DPPH and reducing power assay; anti-inflammatory activities: hemolysis and 15-lipoxygenase (15-LOX) inhibition assay; anticoagulation activities: serine protease inhibition and prothrombin time (PTT) assay of the garlic extract by Pearson square test, where R^2 indicates the correlation coefficient.

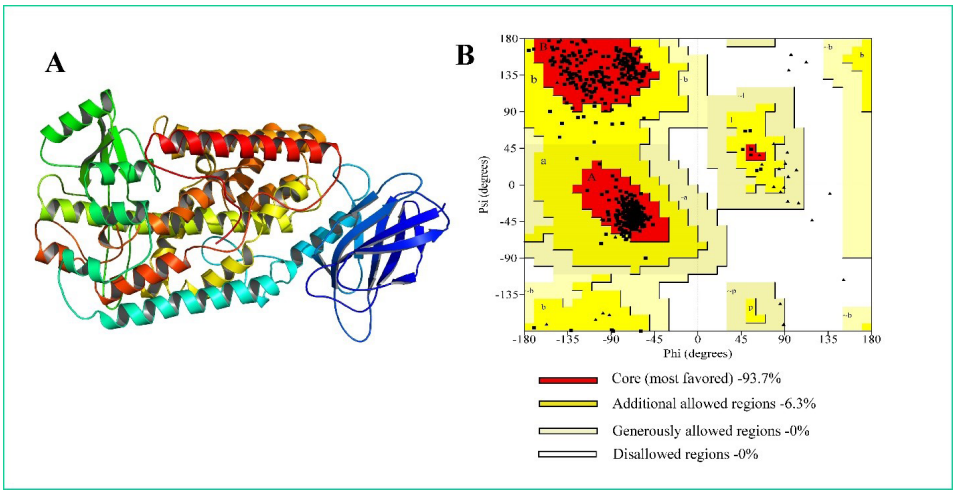

Figure 5. The constructed 15-lipoxygenase -1 (15-LOX1) structure: (A) three-dimensional structure of 15-LOX1 and (B) Ramachandran plot of the protein (15-LOX1).

were selected for each protein based on the docking score compared to Ibuprofen (Figure 6) for further analysis. The top 12 ligands were analyzed for physicochemical and drug-likeness properties. Depending on docking score and ADMET profiling, top 3 compounds were screened for each target protein (Table 1) to analyze the binding stability through MDS. P-coumaric acid (CID: 637542), caffeic acid (CID: 689043), and rhamnetin (CID: 5281691) had greater interaction with 15-LOX1 (Figure 7), whereas cytidine (CID: 6175), cyanidin-3-(6'-malonyl)-glucoside) (CID: 443915), rhamnetin (CID: 5281691) demonstrated substantial binding affinity with 15-LOX2 (Figure 8). The P-L complex structures were evaluated with LigPlot+ by analyzing the respective hydrogen and hydrophobic interactions (Table 2). Figure 9 shows the 2D interaction of the P-L complex with respected hydrogen bonds. The control drug Ibuprofen formed stable interactions with 15-LOX1 and 15-LOX2 through 2 and 3 hydrogen bonds, respectively. On the other hand, P-coumaric acid, caffeic acid, and rhamnetin interacted with 15-LOX1 by

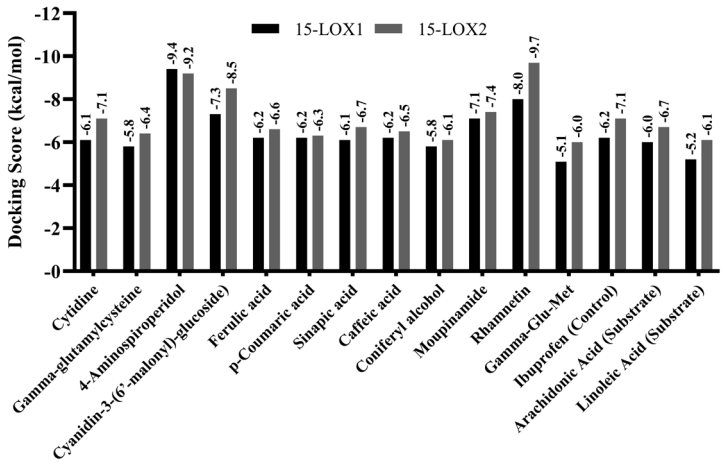

Figure 6. Docking score of the selected phytochemicals along with control (Ibuprofen) and the substrates of 15-lipoxygenase-1 (15-LOX1) and 15-lipoxygenase-2 (15-LOX2).

4 hydrogen bonds each, while cytidine, cyanidin-3-(6'-malonyl)-glucoside), rhamnetin interacted through 6, 5, 3 hydrogen bonds with 15-LOX2, respectively.

MDS analysis

RMSD analysis

The RMSD determines the average structural distance of the atoms of the target protein from its reference position over a certain period. The acceptable range of deviation of the target protein is considered to be 1–3 Å or 0.1–0.3 nm between the frames; however, the deviation beyond this range indicates an extensive structural shift in the protein. The RMSD was evaluated by considering the structures of four ligands: control Ibuprofen (blue), P-coumaric acid (red), caffeic acid (green), and rhamnetin (violet) with the enzyme 15-LOX1 (Figure 10a). Apart from P-coumaric acid, which displayed a slight fluctuation, all other substances had RMSD between 1.1 Å and 3.04 Å. Similarly, the RMSD of the substances: Ibuprofen (blue), cytidine (red), cyanidin-3-(6'-malonyl)-glucoside) (green), and rhamnetin (violet) with the protein 15-LOX2 has been depicted in Figure 11a, where cytidine, cyanidin-3-(6'-malonyl)-glucoside) have shown stable interaction and the RMSD ranged between 1.16 to 2.65 Å. However,

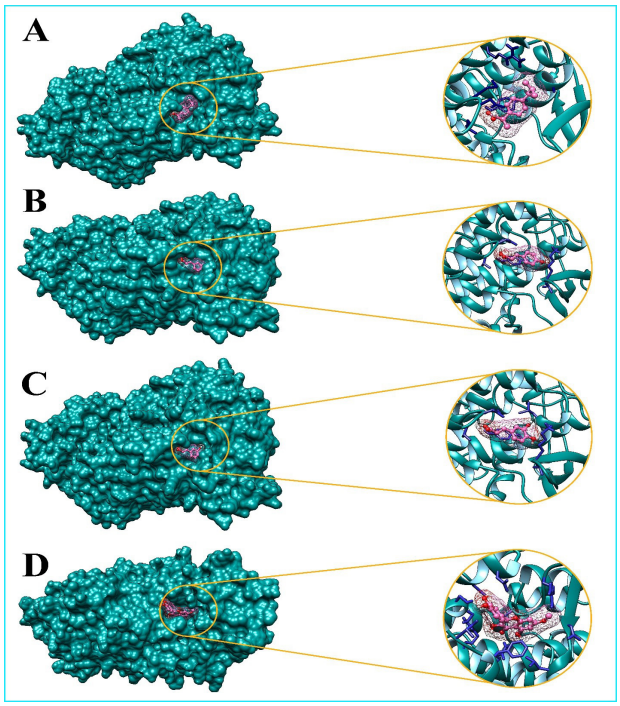

Figure 7. Interaction analysis (3D) of 15-lipoxygenase-1 (15-LOX1) with control Ibuprofen (A), P-coumaric acid (B), Caffeic acid (C), and Rhamnetin (D).

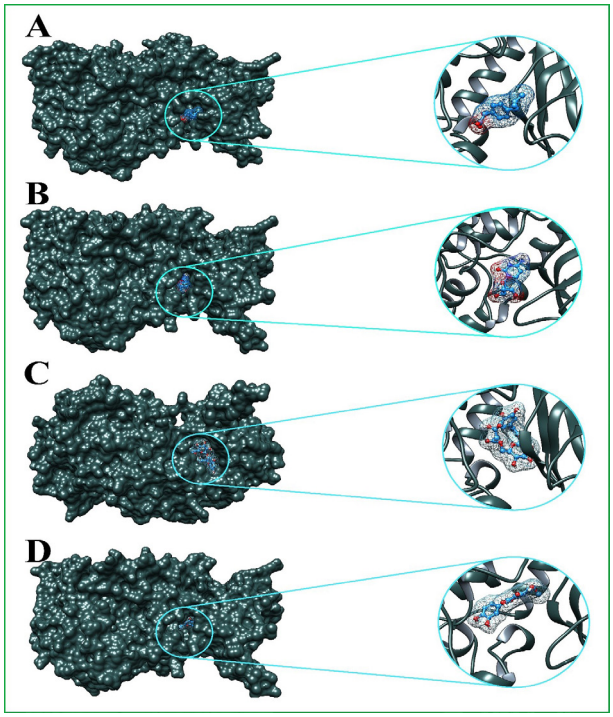

Figure 8. Interaction analysis (3D) of 15-lipoxygenase-2 (15-LOX2) with control Ibuprofen (A), Cytidine (B), Cyanidin-3-(6'-malonyl)-glucoside) (C), and Rhamnetin (D).

Table 1. Absorption, Distribution, Metabolism, Excretion and Toxicity (ADMET) profiling of selected bioactive compounds of garlic

Phytochemicals	PubChem CID	MW (g/mol)	#HA	NRB	HBA	HBD	TPSA (Å²)	iLogP	BBB	IA (% Absorbed)	TC (log mL/min/kg)	LD50 (mol/kg)	HT	AT	NV
Cytidine	6175	243.22	17	2	6	4	130.83	0.32	No	58.476	0.503	1.973	No	No	0
Cyanidin-3-(6′-malonyl)-glucoside)	443915	535.43	38	8	14	8	236.81	2.88	No	18.811	0.66	2.501	No	No	3
Coniferyl alcohol	1549095	180.20	13	3	3	2	49.69	2.16	Yes	91.734	0.233	2.029	No	No	0
Caffeic acid	689043	180.16	13	2	4	3	77.76	0.97	No	69.407	0.508	2.383	No	No	0
Moupinamide	5280537	313.35	23	7	4	3	78.79	2.58	No	90.23	0.27	1.873	Yes	No	0
Rhamnetin	5281691	316.26	23	2	7	4	120.36	2.23	No	80.214	0.473	2.453	No	No	0
Gamma-glutamylcysteine	123938	250.27	16	8	6	4	168.52	0.10	No	1.101	0.321	2.461	No	No	0
4-Aminospiroperidol	195080	410.48	30	6	4	2	78.67	2.82	No	94.274	1.043	2.534	No	No	0
Caffeic acid	689043	180.16	13	2	4	3	77.76	0.97	No	69.407	0.508	2.383	No	No	0
Ferulic acid	445858	194.18	14	3	4	2	66.76	1.62	Yes	93.685	0.623	2.282	No	No	0
Sinapic acid	637775	224.21	16	4	5	2	75.99	1.63	No	93.064	0.718	2.24	No	No	0
Gamma-Glu-Met	7009567	278.33	18	10	6	4	155.02	0.42	No	8.471	0.284	2.434	Yes	No	0
p-Coumaric acid	637542	164.16	12	2	3	2	57.53	0.95	Yes	93.494	0.662	2.155	No	No	0

MW, molecular weight (g/mol); #HA= No. of heavy atoms; NRB = No. of rotatable bonds; HBA, hydrogen bond acceptor; HBD, hydrogen bond donor; TPSA, topological polar surface area; iLogP =The n-octanol/water partition coefficient; BBB, blood-brain barrier; IA, intestinal absorption; TC, total clearance (log mL/min/kg); LD50, oral rat acute toxicity; HT, hepatotoxicity; AT, AMES toxicity; NV= No. of Lipinski's rule violations.

Table 2. Analysis of the binding affinities of top candidate ligands with 15-lipoxygenase -1 (15-LOX1) and 15-lipoxygenase-2 (15-LOX2) compared to the control ligand

Target protein	Pubchem CID	Docking score (k/mol)	Hydrogen bond (Å)	Hydrophobic interaction
15-LOX1	Ibuprofen (CID:3672)	-6.2	MET645(3.25), ASP644(2.87)	ALA255, GLU233, LYS309, LEU226, TYR299, LEU643
	P-coumaric acid (CID:637542)	-6.2	ALA225(2.85), ASP644(2.80), MET645(2.96), TYR229(3.12)	GLY308, LYS309, LEU643
	Caffeic acid (CID:689043)	-6.2	TYR229(3.15), MET645(2.97), ASP644(2.81), ALA225(2.77)	LEU643, LEU226, GLY308, LYS309
	Rhamnetin (CID:5281691)	-8.0	GLN357(2.81), ASP445(3.26), SER438(3.20,2.70)	VAL238, VAL239, ARG241, ASP276, PHE434, THR436, ASP448, SER439
15-LOX2	Ibuprofen (CID:3672)	-7.1	TYR408(3.15), LEU172(3.00), LYS175(2.88)	SER177, ALA13, ARG407, GLY11, GLU12, ARG90, PHE88, TRP109, ASN173
	Cytidine (CID:6175)	-7.1	TRP109(3.16), ARG407(3.02), LEU172(2.70), LYS175(2.97,2.69), TYR408(3.18)	PHE88, TYR176, SER177, ASN173, GLN108, TYR107
	Cyanidin-3-(6′-malonyl)-glucoside) (CID:443915)	-8.5	TRP109(3.18), GLU111(3.20), VAL117(3.19), HIS394(3.16), ARG145(3.18)	MET148, TYR149, ASN173, GLN108, LEU118, GLU141, GLU140, ALA144, LEU116, LEU110, GLY114, THR115
	Rhamnetin (CID:5281691)	-9.7	CYS106(3.06), TYR107(2.75), TYR408(2.74)	HIS627, LEU389, GLN108, ARG145, HIS394, ILE403, ILE174, ARG407, THR406, ASN173, THR385

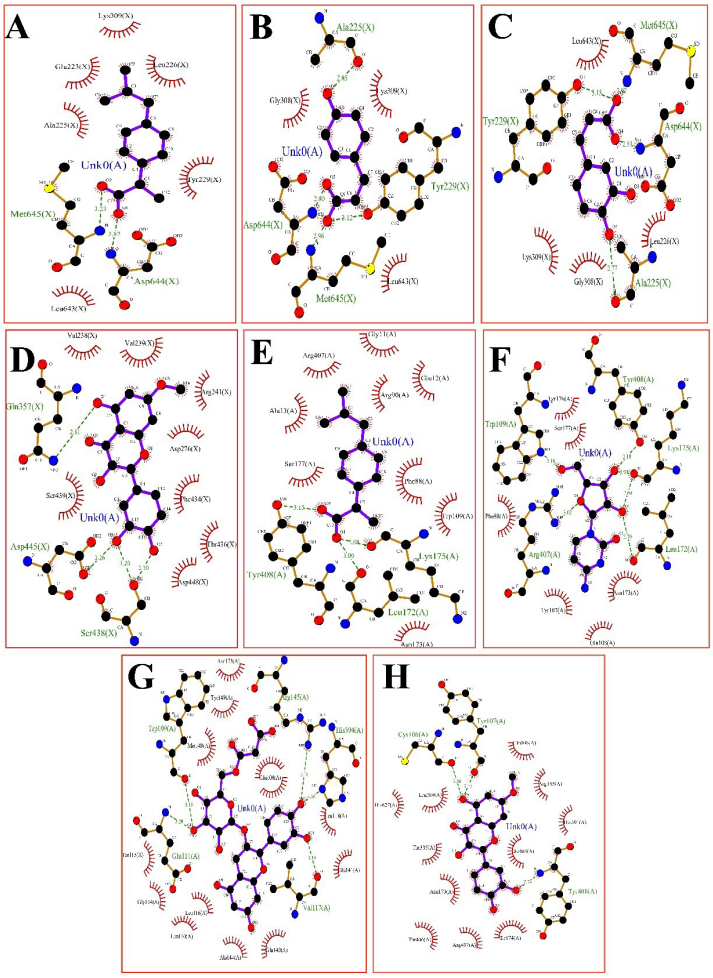

Figure 9. 2D interaction analysis of the ligands and 15-lipoxygenase s (15-LOX1 and 15-LOX2) where (A-D) depicts the interaction of control Ibuprofen (A), P-coumaric acid (B), caffeic acid (C), and rhamnetin (D) with 15-LOX1 and (E-H) depicts the interaction of control Ibuprofen (E), cytidine (F), cyanidin-3-(6'-malonyl)-glucoside) (G) and Rhamnetin (H) with 15-LOX2.

rhamnetin showed higher fluctuation up to 3.48 Å with an average value of 1.97 Å.

RMSF analysis

The RMSF measures how far a protein's amino acid residue has drifted from its initial point over time. It is crucial for protein characterization since it may be used to specify the elasticity and fluctuation of the residues during the simulation. The RMSF of the compounds ibuprofen (blue), P-coumaric acid (red), caffeic acid (green), and rhamnetin (violet) with the enzyme 15-LOX1 is depicted in Figure 10b, where the RMSF value of protein residues ranged from 0.42 to 5.3 Å. Furthermore, Figure 11b depicts RMSF of 15-LOX2 complexed with ibuprofen (blue), cytidine (red), cyanidin-3-(6'-malonyl)-glucoside) (green), and rhamnetin (violet), where the residual fluctuation was found between 0.42 and 5.9 Å. In comparison to 15-LOX1, 15-LOX2 demonstrated greater stability.

Rg analysis

The Rg of an interacting complex can be defined as the arrangement of its atoms around its axis. Since Rg displays the protein compactness during simulation time, determining the Rg is one of the most important criteria for evaluating a macromolecule's structural functioning.

As shown in Figure 10c, the stability of P-coumaric acid, caffeic acid, and rhamnetin, as well as the control ibuprofen, interacted with the targeted protein. 15-LOX1 was investigated in terms of Rg during a 100 ns simulation period, where typical Rg values were in the range of 3.1-4.02 Å. Except for rhamnetin, all P-L complexes had better compactness with Rg up to 3.4 Å. Similarly, in Figure 11c, the Rg of the compounds cytidine, cyanidin-3-(6'-malonyl)-glucoside), rhamnetin, and the control ibuprofen with 15-LOX2 were calculated, where the values ranged between 2.9 and 5.02 Å. Rhamnetin showed the highest Rg value with an average of 4.7Å. Both P-L complexes showed Rg in a considerable range, indicating the binding site has not been faced substantial conformational changes.

Analysis of intramolecular bonds

Throughout 100 ns dynamic simulation, the intramolecular interactions through multiple water bridges and hydrogen,

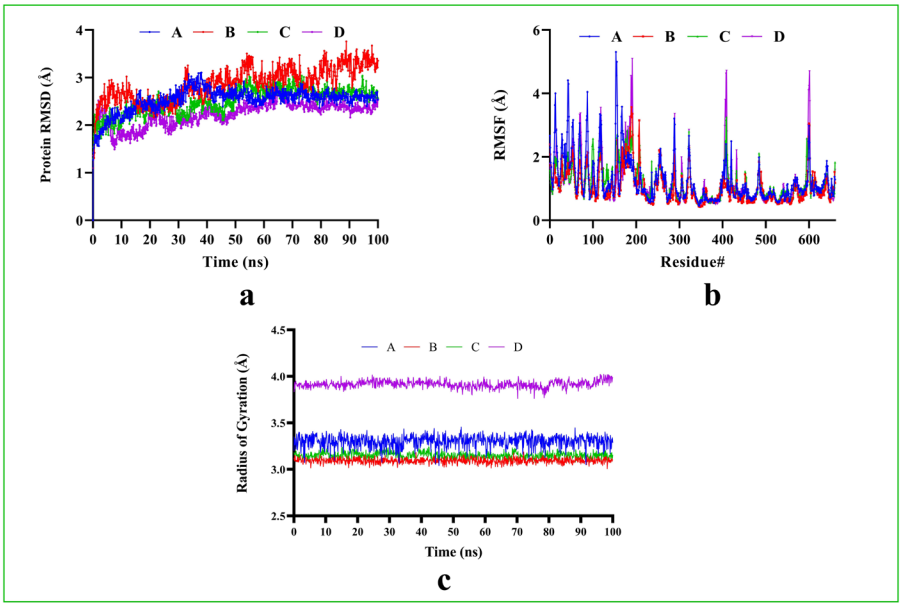

Figure 10. Molecular dynamic simulation (MDS) of 15-lipoxygenase -1 (15-LOX1) complexed with control Ibuprofen (A), P-coumaric acid (B), Caffeic acid (C), and Rhamnetin (D) in respect to the root mean square deviation (RMSD), root mean square fluctuation (RMSF), and radius of gyration (Rg).

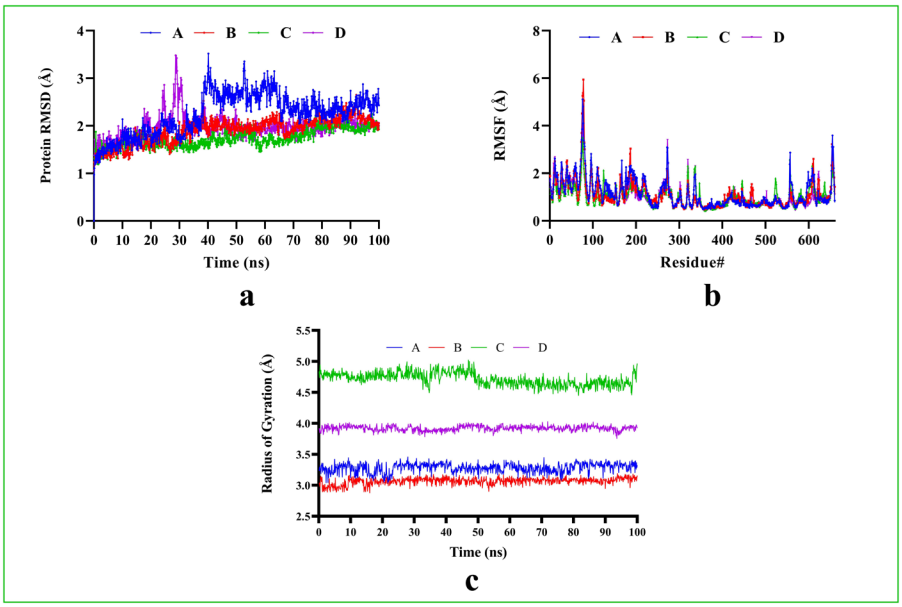

Figure 11. Molecular dynamic simulation (MDS) of 15-LOX2 complexed with control Ibuprofen (A), cytidine (B), cyanidin-3-(6'-malonyl)-glucoside) (C), and rhamnetin (D) in respect to the root mean square deviation (RMSD), root mean square fluctuation (RMSF), and radius of gyration (Rg).

hydrophobic and ionic bonds of P-L complexes have been inspected with the "Simulation Interaction Diagram (SID)" (Figure 12).

Discussion

Elevated ROS level induces oxidative stress, resulting in undesirable changes to cellular components and accelerating several pathogenicities, including protein, lipid, and DNA damage (33). Moreover, the abundance of PUFAs in cell and organelle membranes makes them prone to ROS-induced lipid peroxidation through various enzymatic or non-enzymatic processes that ultimately induce many pro-inflammatory responses. Arachidonic and linoleic acids are the most prevalent PUFAs and act as substrates for LOX enzymes, which catalyze the stereoselective insertion of molecular oxygen to PUFAs to produce hydroperoxyl groups at various carbon positions (34). In different human cells, 5-LOX, 12-LOX, and two forms of 15-LOX (15-LOX1 and 15-LOX2) can effectively transform free arachidonate to 5-hydroperoxy

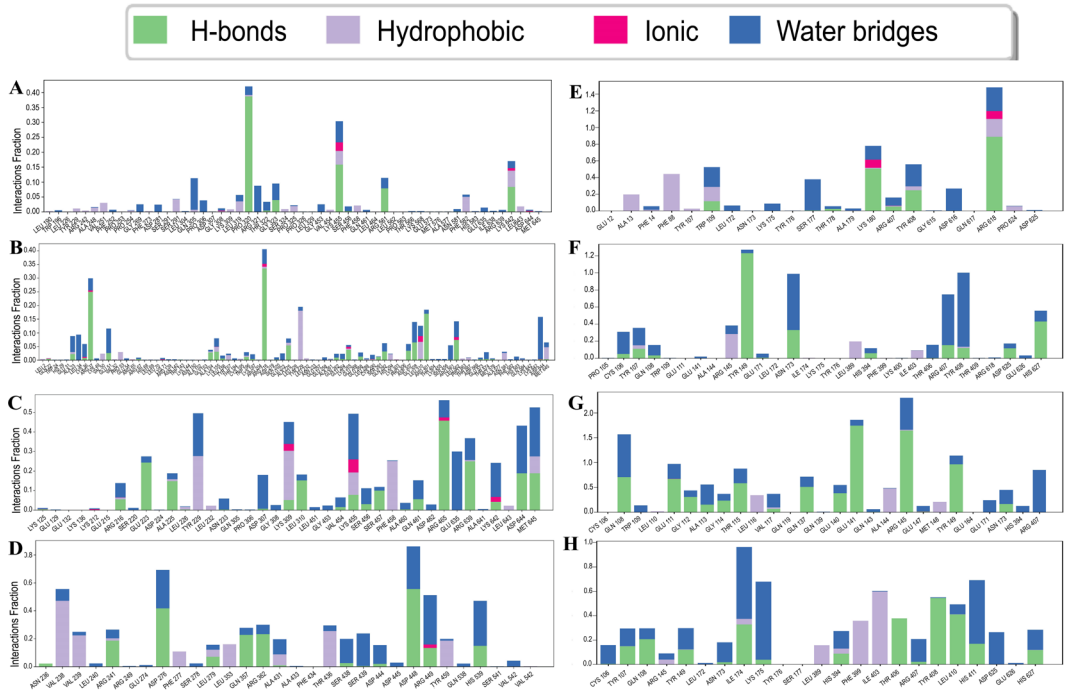

Figure 12. The intramolecular interactions of the 15-lipoxygenases (15-LOX1 and 15-LOX2) with the respective ligands throughout the 100 ns simulation, where (A-D) depicts the interaction of control Ibuprofen (A), P-coumaric acid (B), caffeic acid (C), and Rhamnetin (D) with 15-LOX1 and (E-H) depicts the interaction of control Ibuprofen (E), cytidine (F), cyanidin-3-(6'-malonyl)-glucoside) (G), rhamnetin (H) with 15-LOX2.

eicosatetraenoic acid (5-HPETE), 12-hydroperoxy eicosatetraenoic acid (12-HPETE), 15-hydroperoxy eicosatetraenoic acid (15-HPETE), respectively. HPETEs are further peroxidized to form hydroxyeicosatetraenoic acids and leukotrienes that subsequently induce the expression of pro-inflammatory cytokines, recruit adjacent immune cells, and eventually amplify immunological responses (35). 15-LOX has also been reported to regulate the oxidative alteration of LDL and promote monocyte adhesion to vascular endothelial cells, enhancing the initiation of atherogenicity (36). Oxidative stress also significantly contributes to endothelial damage in the blood vessels, stimulating tissue factor (TF) exposure to the circulatory system and activating the extrinsic pathway-mediated coagulation cascade. Activated factor VII (serine protease) circulates in the blood at a low level and forms a complex with TF (TF-VIIa) that proteolytically activates Factor X to Xa. Factor Xa proteolytically modulates the conversion of prothrombin to thrombin, and thrombin then transforms fibrinogen into fibrin. These events activate the coagulation cascade and increase the production of adhesion molecules, resulting in increased fibrin deposition, impaired fibrinolysis, and eventually accelerating thrombus formation that induces ischemic stroke and cardiovascular complications. (37). Natural antioxidants (secondary metabolites) play a crucial role in neutralizing ROS or inhibiting different oxidative enzymes linked to inflammatory pathways (38). Inflammation related to oxidative stress is a prominent risk factor in the pathophysiology of a wide variety of cardiovascular diseases. Non-steroidal anti-inflammatory drugs are frequently prescribed for various inflammatory diseases having severe adverse effects that have prompted the consideration of developing alternative therapeutic interventions. Therefore, antioxidant metabolites synthesized from plants with anti-inflammatory and anticoagulant effects are indeed effective candidates for commercially available therapeutic medications (38). The aqueous extract of garlic has been demonstrated to have high free radical scavenging activity that inhibits the oxidative alteration of LDLs (39,40) and possesses a potent hepatoprotective effect against oxidative liver injury in rats (41). Several *in vitro* and *in vivo* studies have suggested that garlic's water soluble phytocompounds possess potent antioxidant activity, thereby effectively preventing lipid peroxidation (42,43). In the current study, the aqueous extract of garlic was investigated as a potential source of bioactive compounds by employing different antioxidant, anti-inflammatory, and anticoagulation assays. The DPPH free radical scavenging and reducing power assays are the most frequently used biochemical methods for determining the sample's antioxidant potential (44). In these assays, garlic extract exhibited significant antioxidant activities compared to reference standards, supporting the previous studies revealing that the bioactive elements of the aqueous extract are responsible for its substantial antioxidant effect (45,46). Phenolics, flavonoids, tannins and other polyphenolic metabolites have been extensively researched as the principal free radical scavengers in a wide variety of plant species. Proton loss and free radical

neutralization are the key mechanisms through which phenolic substances exhibit antioxidant effects (47). Moreover, it has been reported that the polyphenolic metabolites derived from plants also exhibit high anti-inflammatory as well as anticoagulant properties (48). In this study, the aqueous extract possessed a significant concentration of phenols and flavonoids, indicating the strong antioxidant activity of garlic. This finding supports the evidence of the previous studies (12,49).

The anti-inflammatory effect of the aqueous extract was assessed by employing two distinct strategies (hypotonicity-induce hemolysis assay, 15-LOX inhibition assay) in this study. In the hypotonicity-induce hemolysis assay, human RBCs were used as a source of plasma membranes since they do not possess nuclei or internal membranes, making them an ideal source for biochemical investigations (50). Moreover, most anti-inflammatory drugs work by stabilizing the lysosomal membrane to reduce the secretion of proteolytic enzymes to the surrounding tissues, hence inhibiting the onset of inflammatory conditions (51). In this study, different concentrations of the aqueous garlic extract were used to protect the lysis of the RBC membrane, wherein the extract was found to have a potent inhibitory effect in preventing hemolysis at a comparatively lower concentration with respect to the standard Aspirin. Based on the aforementioned features, the aqueous extract was picked for further investigation for the inhibition of the pro-inflammatory pathway. The determination of anti-inflammatory activity through *in vitro* soybean 15-LOX inhibition assay was significant since this enzyme utilizes arachidonic acid or linolic acid as its substrate and the active site is closely identical to that of human LOX, which effectively modulates the synthesis of pro-inflammatory mediators such as leukotrienes from the lipid peroxidation cascade (52). Several studies have been performed to explore the anti-inflammatory effects of various garlic extracts; however, few researches have been conducted to analyze the 15-LOX inhibitory activity of garlic to identify its anti-inflammatory potential. For this purpose, soybean 15-LOX inhibition assay was conducted to evaluate the effectiveness of aqueous garlic extract in preventing chronic inflammation by inhibiting enzymatic peroxidation of PUFAs. The aqueous extract demonstrated a considerable LOX inhibitory effect compared to standard Quercetin. The anti-inflammatory efficacy of the extracts was likewise consistent with that of the antioxidant properties. The anticoagulation property of garlic was evaluated by *in vitro* serine protease (Trypsin) inhibition assay and PTT assay. Trypsin belongs to the group of serine proteases that are critical for maintaining pathophysiological processes in the body, including extrinsic blood coagulation cascade, inflammation, apoptosis, and so on (53,54). The intervention of such diseases with natural protease inhibitors is thus an attractive target for pharmacological research (55). The aqueous extract revealed substantial serine protease inhibition activity with a minimal concentration with respect to the standard Quercetin in this study. In the PTT assay, the anticoagulation effect was assessed by determining the coagulation times at aliquots of various concentrations of the extracts. The aqueous extract exhibited a higher clotting time in comparison to the standard warfarin. It has been reported that organosulfur compounds and phenolic contents of garlic extract are responsible for its high anticoagulant effect (56). The one-tailed t-test was performed to statistically analyze the negative control and test sample data to assess the significance level of garlic extract for each concentration of all *in vitro* assays. All *P* values less than 0.033 substantiate significant differences between the group means of the test samples and control, indicating that this difference is not due to random data sampling. A linear relationship was observed among antioxidant, anticoagulation, and anti-inflammatory activities of the test sample. The R squared values generated from the correlation analysis close to +1 substantiate that the relationship is strong. Previous studies evidently suggested that polyphenols and polyphenol-rich extracts simultaneously show antioxidative, anticoagulant, and anti-inflammatory properties (57). Hence, the linearity in correlation supports that the polyphenol molecules might contribute to the antioxidant, anti-inflammatory, and anticoagulation activities in the aqueous garlic extract.

Further, *in silico* molecular docking and MDS analysis of reported small compounds of garlic against 15-LOX1 and 15-LOX2 were performed to figure out the most efficient phytochemical ligands and validate the anti-inflammatory potential. All top three selected compounds for each target enzyme showed stronger interactions than the substrates: arachidonic and linolic acid (Figure 6). Considering the MDS analysis of 15-LOX1, all the tested compounds except P-coumaric acid showed greater stability in all three parameters. On the other hand, cytidine, cyanidin-3-(6'-malonyl)-glucoside), and rhamnetin exhibited consistent interaction with 15-LOX2 throughout the 100 ns simulation. Depending upon molecular docking and dynamic simulation, rhamnetin was selected as a potential compound that could efficiently block both 15-LOX1 and 15-LOX2. Several *in vivo* studies also support the anti-inflammatory potential of this compound (58). Rhamnetin was reported to down-regulate the release of pro-inflammatory mediators such as tumor necrosis factor (TNF-α) and macrophage inflammatory proteins (MIPs) in a lipopolysaccharide-induced mouse macrophage cell line (59). Hence, rhamnetin would alleviate inflammation-related complications and act as a major biopharmaceutical to prevent 15-LOX mediated inflammatory diseases.

Conclusion

Garlic (*A. sativum*) is extensively used for its distinct flavor and potential health benefits including hypocholesterolemic, thrombolytic, and antioxidant

properties. For that purpose, this study aimed to investigate the different bioactive properties of the aqueous extract of garlic. According to the findings of the biochemical assays, the aqueous extract comprises a high concentration of polyphenolic components that manifest significant antioxidant potential along with strong anti-inflammatory and anticoagulant effects. Further comprehensive analysis of garlic to explore its pharmacological activity can contribute to isolating potent pharma and nutraceuticals responsible for the relevant bioactivities.

Acknowledgments

The authors would like to express their utmost gratitude to Mr. Kumar Shubhro, Prof. Dr. SM Mahbubur Rahman from Biotechnology and Genetic Engineering Discipline, Khulna University for their technical and intellectual assistance throughout the duration of this study.

Authors' contribution

AMK and MdAS designed the methodology, conducted experiments, prepared visuals and wrote the initial draft; MdHR, PB, and MdNH assisted in the computational section of the study; RS and SM conducted formal analysis, validated the data, reviewed and edited the manuscript; MdEI, KMDI and MdMB conceptualized and supervised the project. All authors discussed the results and agreed on the final manuscript.

Conflict of interests

The authors have no conflicts of interest to declare.

Ethical considerations

The Khulna University Research Cell's ethical code (KUAEC-2017/08/14) was followed for the biochemical experiments that involved human participants.

Funding/Support

Khulna University Research Cell, Khulna University, Bangladesh (Grant Number: KURC-RGP-11/2019) supported this research.

References

1. Poggi C, Dani C. Antioxidant strategies and respiratory disease of the preterm newborn: an update. Oxid Med Cell Longev. 2014;2014:721043. doi: 10.1155/2014/721043.
2. Lushchak VI. Free radicals, reactive oxygen species, oxidative stress and its classification. Chem Biol Interact. 2014;224:164-75. doi: 10.1016/j.cbi.2014.10.016.
3. Umeno A, Biju V, Yoshida Y. In vivo ROS production and use of oxidative stress-derived biomarkers to detect the onset of diseases such as Alzheimer's disease, Parkinson's disease, and diabetes. Free Radic Res. 2017;51(4):413-27. doi: 10.1080/10715762.2017.1315114.
4. van Leyen K, Arai K, Jin G, Kenyon V, Gerstner B, Rosenberg PA, et al. Novel lipoxygenase inhibitors as neuroprotective reagents. J Neurosci Res. 2008;86(4):904-9. doi: 10.1002/jnr.21543.
5. Ackermann JA, Hofheinz K, Zaiss MM, Krönke G. The double-edged role of 12/15-lipoxygenase during inflammation and immunity. Biochim Biophys Acta Mol Cell Biol Lipids. 2017;1862(4):371-81. doi: 10.1016/j.bbalip.2016.07.014.
6. Dey D, Paul PK, Al Azad S, Al Mazid MF, Khan AM, Sharif MA, et al. Molecular optimization, docking, and dynamic simulation profiling of selective aromatic phytochemical ligands in blocking the SARS-CoV-2 S protein attachment to ACE2 receptor: an in silico approach of targeted drug designing. J Adv Vet Anim Res. 2021;8(1):24-35. doi: 10.5455/javar.2021.h481.
7. Phan ADT, Netzel G, Chhim P, Netzel ME, Sultanbawa Y. Phytochemical characteristics and antimicrobial activity of Australian grown garlic (*Allium Sativum* L.) Cultivars. Foods. 2019;8(9):358. doi: 10.3390/foods8090358.
8. Bozin B, Mimica-Dukic N, Samojlik I, Goran A, Igic R. Phenolics as antioxidants in garlic (*Allium sativum* L., Alliaceae). Food Chem. 2008;111(4):925-9. doi: 10.1016/j.foodchem.2008.04.071.
9. Iciek M, Kwiecień I, Włodek L. Biological properties of garlic and garlic-derived organosulfur compounds. Environ Mol Mutagen. 2009;50(3):247-65. doi: 10.1002/em.20474.
10. Goncagul G, Ayaz E. Antimicrobial effect of garlic (*Allium sativum*). Recent Pat Antiinfect Drug Discov. 2010;5(1):91-3. doi: 10.2174/157489110790112536.
11. Jang HJ, Lee HJ, Yoon DK, Ji DS, Kim JH, Lee CH. Antioxidant and antimicrobial activities of fresh garlic and aged garlic by-products extracted with different solvents. Food Sci Biotechnol. 2018;27(1):219-25. doi: 10.1007/s10068-017-0246-4.
12. Chen S, Shen X, Cheng S, Li P, Du J, Chang Y, et al. Evaluation of garlic cultivars for polyphenolic content and antioxidant properties. PLoS One. 2013;8(11):e79730. doi: 10.1371/journal.pone.0079730.
13. Nazir I, Chauhan RS. Qualitative phytochemical analysis of *Allium sativum* (Garlic) and *Curcuma longa* (Turmeric). J Entomol Zool Stud. 2019;7(1):545-7.
14. Indrasanti D, Indradji M, Hastuti S, Aprilliyani E, Fatikha F, Rosyadi KA. The administration of garlic extract on *Eimeria stiedai* oocysts and the hematological profile of the coccidia infected rabbits. Media Peternakan. 2017;40(3):158-64. doi: 10.5398/medpet.2017.40.3.158.
15. Udu-Ibiam OE, Ogbu O, Ibiam UA, Nnachi AU, Agah MV, Ukaegbu CO, et al. Phytochemical and antioxidant analyses of selected edible mushrooms, ginger and garlic from Ebonyi State, Nigeria. IOSR J Pharm Biol Sci. 2014;9(3):86-91. doi: 10.9790/3008-09348691.
16. Tavares L, Santos L, Zapata Noreña CP. Bioactive compounds of garlic: a comprehensive review of encapsulation technologies, characterization of the encapsulated garlic compounds and their industrial applicability. Trends Food Sci Technol. 2021;114:232-44. doi: 10.1016/j.tifs.2021.05.019.
17. Shang A, Cao SY, Xu XY, Gan RY, Tang GY, Corke H, et al. Bioactive compounds and biological functions of garlic (*Allium sativum* L.). Foods. 2019;8(7):246. doi: 10.3390/foods8070246.
18. Brand-Williams W, Cuvelier ME, Berset C. Use of a free radical method to evaluate antioxidant activity. LWT Food Sci Technol. 1995;28(1):25-30. doi: 10.1016/s0023-6438(95)80008-5.

19. Afrin S, Pervin R, Sabrin F, Rony SR, Sohrab M, Islam M, et al. In vitro antioxidant activity, antimicrobial and preliminary cytotoxic activity of *Cynometra ramiflora*-a mangrove plant. J Microbiol Biotechnol Food Sci. 2016;6(2):844-50. doi: 10.15414/jmbfs.2016.6.2.844-850.
20. Aunjum A, Biswas R, Nurunnabi TR, Rahman SM, Billah MM, Islam ME, et al. Antioxidant and antibacterial activity of three herbs belonging to *Zingiber* genus of Bangladesh. Adv Tradit Med. 2020;20(3):343-50. doi: 10.1007/s13596-019-00403-y.
21. Yesmin S, Paul A, Naz T, Rahman AB, Akhter SF, Wahed MI, et al. Membrane stabilization as a mechanism of the anti-inflammatory activity of ethanolic root extract of Choi (*Piper chaba*). Clin Phytosci. 2020;6(1):59. doi: 10.1186/s40816-020-00207-7.
22. Wangensteen H, Samuelsen AB, Malterud KE. Antioxidant activity in extracts from coriander. Food Chem. 2004;88(2):293-7. doi: 10.1016/j.foodchem.2004.01.047.
23. Kunitz M. Crystalline soybean trypsin inhibitor: II. General properties. J Gen Physiol. 1947;30(4):291-310. doi: 10.1085/jgp.30.4.291.
24. Biswas R, Rahman SMM, Islam KM, Billah MM, Aunjum A, Nurunnabi TR, et al. Antioxidant, anti-inflammatory, and anticoagulation properties of *Aegiceras corniculatum* and *Acanthus ilicifolius*. Pharm Biomed Res. 2019;5(3):35-44. doi: 10.18502/pbr.v5i3.2117.
25. Wu F, Xu J. Deep template-based protein structure prediction. PLoS Comput Biol. 2021;17(5):e1008954. doi: 10.1371/journal.pcbi.1008954.
26. Elengoe A, Sundramoorthy ND. Molecular docking of curcumin with breast cancer cell line proteins. Pharm Biomed Res. 2020;6(1):27-36. doi: 10.18502/pbr.v6i1.3425.
27. Pettersen EF, Goddard TD, Huang CC, Couch GS, Greenblatt DM, Meng EC, et al. UCSF Chimera--a visualization system for exploratory research and analysis. J Comput Chem. 2004;25(13):1605-12. doi: 10.1002/jcc.20084.
28. Sharif MA, Hossen MS, Shaikat MM, Haidary FM, Ema TI, Dey D, et al. Molecular optimization, docking and dynamic simulation study of selective natural aromatic components to block E2-CD81 complex formation in predating protease inhibitor resistant HCV influx. Int J Pharm Res. 2021;13(2):3511-25. doi: 10.31838/ijpr/2021.13.02.408.
29. Bushra R, Aslam N. An overview of clinical pharmacology of Ibuprofen. Oman Med J. 2010;25(3):155-1661. doi: 10.5001/omj.2010.49.
30. Daina A, Michielin O, Zoete V. SwissADME: a free web tool to evaluate pharmacokinetics, drug-likeness and medicinal chemistry friendliness of small molecules. Sci Rep. 2017;7:42717. doi: 10.1038/srep42717.
31. Pires DE, Blundell TL, Ascher DB. pkCSM: predicting small-molecule pharmacokinetic and toxicity properties using graph-based signatures. J Med Chem. 2015;58(9):4066-72. doi: 10.1021/acs.jmedchem.5b00104.
32. Biswas P, Dey D, Rahman A, Islam MA, Susmi TF, Kaium MA, et al. Analysis of SYK gene as a prognostic biomarker and suggested potential bioactive phytochemicals as an alternative therapeutic option for colorectal cancer: an in-silico pharmaco-informatics investigation. J Pers Med. 2021;11(9):888. doi: 10.3390/jpm11090888.
33. Su LJ, Zhang JH, Gomez H, Murugan R, Hong X, Xu D, et al. Reactive oxygen species-induced lipid peroxidation in apoptosis, autophagy, and ferroptosis. Oxid Med Cell Longev. 2019;2019:5080843. doi: 10.1155/2019/5080843.
34. Kuhn H, Banthiya S, van Leyen K. Mammalian lipoxygenases and their biological relevance. Biochim Biophys Acta. 2015;1851(4):308-30. doi: 10.1016/j.bbalip.2014.10.002.
35. Salekeen R, Mou SN, Islam ME, Ahmed A, Billah MM, Rahman SM, et al. Predicting multi-enzyme inhibition in the arachidonic acid metabolic network by *Heritiera fomes* extracts. J Biomol Struct Dyn. 2022;40(9):4259-72. doi: 10.1080/07391102.2020.1855248.
36. Funk CD. Lipoxygenase pathways as mediators of early inflammatory events in atherosclerosis. Arterioscler Thromb Vasc Biol. 2006;26(6):1204-6. doi: 10.1161/01.ATV.0000222960.43792.ff.
37. Lopes-Pires ME, Frade-Guanaes JO, Quinlan GJ. Clotting dysfunction in sepsis: a role for ROS and potential for therapeutic intervention. Antioxidants (Basel). 2021;11(1):88. doi: 10.3390/antiox11010088.
38. Islam ME, Rahman SM, Sohrab MH, Biswas R, Ullah MS, Islam KD. Concordance of antioxidant and anti-Inflammatory activity in *Xylocarpus granatum* (Koen). J Bangladesh Agric Univ. 2019;17(4):466-75. doi: 10.3329/jbau.v17i4.44607.
39. Lewin G, Popov I. Antioxidant effects of aqueous garlic extract. 2nd communication: Inhibition of the Cu(2+)-initiated oxidation of low density lipoproteins. Arzneimittelforschung. 1994;44(5):604-7.
40. Ide N, Nelson AB, Lau BH. Aged garlic extract and its constituents inhibit Cu(2+)-induced oxidative modification of low density lipoprotein. Planta Med. 1997;63(3):263-4. doi: 10.1055/s-2006-957668.
41. Sener G, Sehirli O, Ipçi Y, Ercan F, Sirvanci S, Gedik N, et al. Aqueous garlic extract alleviates ischaemia-reperfusion-induced oxidative hepatic injury in rats. J Pharm Pharmacol. 2005;57(1):145-50. doi: 10.1211/0022357055209.
42. Arhan M, Oztürk HS, Turhan N, Aytac B, Güven MC, Olcay E, et al. Hepatic oxidant/antioxidant status in cholesterol-fed rabbits: effects of garlic extract. Hepatol Res. 2009;39(1):70-7. doi: 10.1111/j.1872-034X.2008.00401.x.
43. Rasul Suleria HA, Sadiq Butt M, Muhammad Anjum F, Saeed F, Batool R, Nisar Ahmad A. Aqueous garlic extract and its phytochemical profile; special reference to antioxidant status. Int J Food Sci Nutr. 2012;63(4):431-9. doi: 10.3109/09637486.2011.634786.
44. Pisoschi AM, Pop A, Cimpeanu C, Predoi G. Antioxidant capacity determination in plants and plant-derived products: a review. Oxid Med Cell Longev. 2016;2016:9130976. doi: 10.1155/2016/9130976.
45. Queiroz YS, Ishimoto EY, Bastos DH, Sampaio GR, Torres EA. Garlic (*Allium sativum* L.) and ready-to-eat garlic products: in vitro antioxidant activity. Food Chem. 2009;115(1):371-4. doi: 10.1016/j.foodchem.2008.11.105.
46. Wang X, Liu R, Yang Y, Zhang M. Isolation, purification and identification of antioxidants in an aqueous aged garlic extract. Food Chem. 2015;187:37-43. doi: 10.1016/j.foodchem.2015.03.109.
47. Shahidi F, Ambigaipalan P. Phenolics and polyphenolics in foods, beverages and spices: antioxidant activity and health effects–a review. J Funct Foods. 2015;18(Pt B):820-97. doi: 10.1016/j.jff.2015.06.018.
48. Gueboudji Z, Addad D, Kadi K, Nagaz K, Secrafi M, Yahya LB, et al. Biological activities and phenolic compounds of olive oil mill wastewater from Abani, endemic Algerian variety. Sci Rep. 2022;12(1):6042. doi: 10.1038/s41598-022-

10052-y.
49. Elosta A, Slevin M, Rahman K, Ahmed N. Aged garlic has more potent antiglycation and antioxidant properties compared to fresh garlic extract in vitro. Sci Rep. 2017;7:39613. doi: 10.1038/srep39613.
50. Amujoyegbe OO, Agbedahunsi JM, Akinpelu BA, Oyedapo OO. In vitro evaluation of membrane stabilizing activities of leaf and root extracts of *Calliandra portoricensis* (Jacq.) Benth on sickle and normal human erythrocytes. Int Res J Pharm Pharmacol. 2012;2(8):198-203.
51. Navale G, Patil DD, Patil AA, Patil KB, Patil NB. Membrane stabilization assay for anti-inflammatory activity yields misleading results for samples containing traces of methanol. Asian J Pharm Res. 2019;9(3):169-71. doi: 10.5958/2231-5691.2019.00026.1.
52. Kim MY, Kim YC, Chung SK. Identification and in vitro biological activities of flavonols in garlic leaf and shoot: inhibition of soybean lipoxygenase and hyaluronidase activities and scavenging of free radicals. J Sci Food Agric. 2005;85(4):633-40. doi: 10.1002/jsfa.1899.
53. Jiang L, Yuan C, Huang M. A general strategy to inhibit serine protease by targeting its autolysis loop. FASEB J. 2021;35(2):e21259. doi: 10.1096/fj.202002139RR.
54. Heutinck KM, ten Berge IJ, Hack CE, Hamann J, Rowshani AT. Serine proteases of the human immune system in health and disease. Mol Immunol. 2010;47(11-12):1943-55. doi: 10.1016/j.molimm.2010.04.020.
55. Shahwar D, Raza MA, Shafiq-Ur-Rehman, Abbasi MA, Atta-Ur-Rahman. An investigation of phenolic compounds from plant sources as trypsin inhibitors. Nat Prod Res. 2012;26(12):1087-93. doi: 10.1080/14786419.2011.559637.
56. Lamponi S. Bioactive natural compounds with antiplatelet and anticoagulant activity and their potential role in the treatment of thrombotic disorders. Life. 2021;11(10):1095. doi: 10.3390/life11101095.
57. Yahfoufi N, Alsadi N, Jambi M, Matar C. The immunomodulatory and anti-inflammatory role of polyphenols. Nutrients. 2018;10(11):1618. doi: 10.3390/nu10111618.
58. Wang M, Wu Y, Li W. Rhamnetin ameliorates macrophage-mediated inflammation and pro-atherosclerosis pathways in apolipoprotein E-deficient mice. J Physiol Pharmacol. 2021;72(2):249-58. doi: 10.26402/jpp.2021.2.10.
59. Jnawali HN, Lee E, Jeong KW, Shin A, Heo YS, Kim Y. Anti-inflammatory activity of rhamnetin and a model of its binding to c-Jun NH2-terminal kinase 1 and p38 MAPK. J Nat Prod. 2014;77(2):258-63. doi: 10.1021/np400803n.